Multiple foci and a long filament observed with focused femtosecond pulse propagation in fused silica

Article *in* Optics Letters · March 2002

DOI: 10.1364/OL.27.000448 · Source: PubMed

Multiple foci and a long filament observed with focused femtosecond pulse propagation in fused silica

Zhaoxin Wu, Hongbing Jiang,* Le Luo, Hengchang Guo, Hong Yang, and Qihuang Gong

Department of Physics & State Key Laboratory for Mesoscopic Physics, Peking University, Beijing 100871, China

Received October 17, 2001

Multiple foci and a long filament are observed when we focus a femtosecond laser pulse into a fused-silica sample. The dependences of the intensity distribution of the plasma luminescence on the pulse energy and the numerical aperture (NA) of the focusing objective are investigated. Multiple foci are observed when NA of ≤ 0.65. A long filament tail is formed instead of multiple foci when the NA is 0.85. A physical image of femtoseond pulse propagation is given by a model based on the nonlinear Schrödinger equation. © 2002 Optical Society of America

OCIS codes: 190.5530, 190.7110, 220.4000, 320.7130.

Theoretical and experimental investigations of the nonlinear propagation of an ultrashort laser pulse through a transparent medium have been the subjects of numerous studies in the past three decades, because nonlinear propagation is accompanied by many interesting phenomena, such as changes in the temporal, spatial, and spectral properties of the laser pulse. For femtosecond pulses, pulse propagation in filaments with lengths of tens of meters in air,[1–3] supercontinuum generation,[4] pulse splitting,[5] conical emission,[2,3] and refocusing[6] were observed. In a dielectric solid, the filament that is formed can possibly be used for applications such as waveguides,[7,8] three-dimensional optical storage,[9] and microfabrication.[10] However, to our knowledge, the interaction between a single focused femtosecond pulse and a condensed medium has not been studied systematically, and so it is necessary to investigate the propagation characteristics and the corresponding fundamental nonlinear dynamics.

In this Letter the behavior of single focused femtosecond pulse propagation in fused silica is studied in detail. The phenomenon of multiple foci was clearly observed. The dependences of multiple foci on the pulse energy and the numerical aperture (NA) of the microscope objective were studied. Instead of refocusing, a filament occurred when the NA of the objective was greater than 0.85. To interpret the experimental results, Wagner *et al.*[11] solved the nonlinear Schrödinger equation with a method that had been used in self-trapping, taking into consideration multiphoton ionization, plasma absorption, and defocusing by plasma. Compared with this numerical simulation of the nonlinear Schrödinger equation, our analysis gives a clearer picture of pulse propagation in a transparent medium, which is analogous to the movement of a classical particle in a potential well.

A Ti:sapphire chirped-pulse-amplification laser with a pulse duration of 120 fs and a wavelength of 800 nm was used in our experiment. The repetition rate of the laser was 10 Hz. Figure 1 shows a schematic of the experimental setup. Interaction of a single pulse with the fused silica was achieved with a shutter during the exposure time of the CCD camera. We employed a spatial filter to obtain a high-quality beam. We chose objectives with NAs of 0.15, 0.40, 0.65, and 0.85 to focus the laser. The surfaces of the fused-silica sample were polished, and the size of the sample was 5 mm $\times$ 5 mm $\times$ 3 mm. The energy of the input laser pulse was monitored by a calibrated photodiode. The plasma luminescence was imaged on a CCD camera by another objective. The intensity of the plasma luminescence could be qualitatively characterized by the intensity distribution of the incident pulse in the focal region,[6] so the multiple peaks of the intensity of the plasma luminescence reflect the refocusing effect of the laser beam.

Figures 2–4 show the images and the on-axis intensity distributions of the plasma luminescence when objectives with NAs of 0.15, 0.40, and 0.85 were used to focus the laser pulse with different input energies. The measured waist, w_0, of the laser beam with objectives of NA 0.15, 0.40, and 0.85 is approximately 2.8, 1.3, and 1.0 μm, respectively, and the corresponding Rayleigh lengths are approximately 30.8, 9.5, and 5.5 μm.

For all the objectives, when the pulse energy is lower, there is only one focus, as shown in Figs. 2(a), 3(a), and 4(a). As the energy is increased, a second focus appears for 0.15 and 0.40 NA, as shown in Figs. 2(b) and 3(b), respectively. For 0.40 NA, a third focus appears as the energy is increased more, as shown in Figs. 3(c) and 3(d). When the 0.65-NA objective is used to focus the beam, the resulting images of the plasma and the on-axis intensity distribution of plasma luminescence are similar to those shown in Fig. 3. However, for the 0.85 NA, there is not multiple foci but a long filament at a higher pulse energy, as shown in Fig. 4. In Fig. 2, the distance between two peaks is 15 μm,

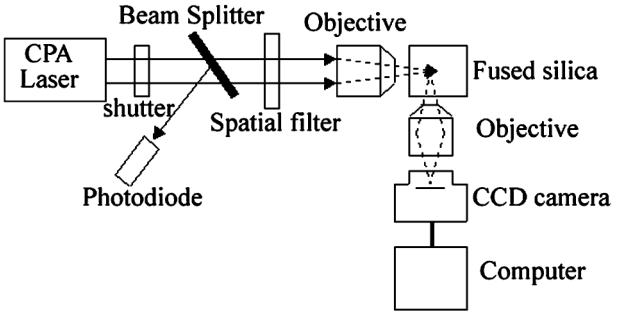

Fig. 1. Experimental setup. CPA, chirped-pulse amplification.

0146-9592/02/060448-03$15.00/0

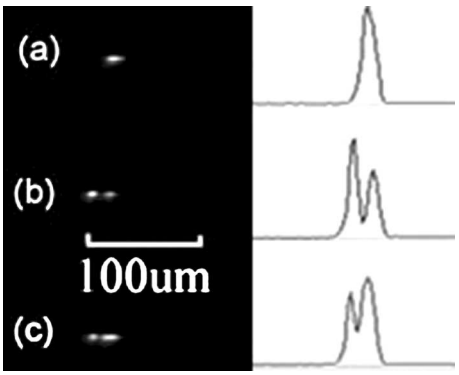

Fig. 2. Photomicrographs and on-axis relative intensities of the plasma luminescence at different pulse energies: (a) 0.80 μJ, (b) 140 μJ, (c) 1.61 μJ. The NA of the objective is 0.15.

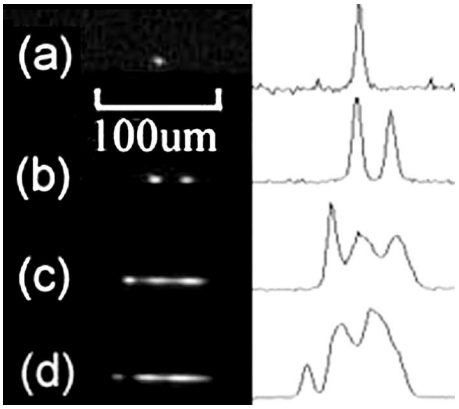

Fig. 3. Photomicrographs and on-axis relative intensities of the plasma luminescence at different pulse energies: (a) 0.27 μJ, (b) 0.35 μJ, (c) 0.55 μJ, (d) 0.95 μJ. The NA of the objective is 0.40.

which is smaller than the distance between two peaks in Fig. 3(b), which is 23 μm. In Figs. 3(c) and 3(d), the distance between the first and second peaks is smaller than that between the second and third peaks. It is clear that the filaments move upstream with higher input-pulse energy in Figs. 2–4, which indicates that self-focusing is important for a NA with an objective of $\leq$0.85.

The underlying physical mechanism for the filamentation is the dynamic competition between self-focusing by the Kerr effect and defocusing by the plasma. A physical model was developed for intense pulse propagation in fused silica, which was studied previously for laser-induced breakdown and propagation in gas[12] and air.[13]

$$\left(i2k\frac{\partial}{\partial z}+\nabla_{\perp}{}^2\right)E = kk''\frac{\partial^2 E}{\partial \xi^2} - ik\sigma(1+i\omega\tau)\rho E - ik\beta^K|E|^{2K-2}E - 2kk_0n_2|E|^2E, \quad (1)$$

$$\frac{\partial \rho}{\partial \xi} = \frac{1}{n_b{}^2}\frac{\sigma}{E_g}\rho|E|^2 + \frac{\beta^{(K)}|E|^{2K}}{K\hbar\omega} - a\rho^2. \quad (2)$$

Equation (1) is the nonlinear Schrödinger equation including the effects of self-focusing, multiphoton absorption, group-velocity dispersion and absorption, and defocusing by the plasma. Equation (2) is a coupled equation that comes from the Drude model. $E(r, z, \xi)$ is the electric field envelope expressed in the retarded coordinate system; $\xi = t - z/\nu_g$; ν_g is the group velocity; and ω and $|E|^2$ are the frequency and the intensity of the laser, respectively. Also, $k = n_b\omega/c$, $k'' = \partial^2 k/\partial\omega^2$, ρ is the electron density, σ is the cross section for the inverse bremsstrahlung, $\sigma = (ke^2\tau')/\{\omega m_e\epsilon_0[1+(\omega\tau')^2]\}$,[13] the electron collision time $\tau' = 1.0\times10^{-15}$ s, and $\beta^{(K)}$ is the K-photon absorption coefficient. The critical power for self-focusing is $P_{cr} = 0.159\lambda_0{}^2/n_bn_2$.[13] The parameters of our samples are $n_b = 1.46$, $K = 6$, $n_2 = 2.5\times10^{-16}$ cm^2/W, and $\beta^{(6)} = 6.1\times10^{-63}$ cm^{11} W^{-6}.

To get semianalytical solutions of Eqs. (1) and (2) for a clear image of femtosecond pulse propagation, we neglect group-velocity dispersion, avalanche ionization, and electron recombination, and paraxial approximation is adopted. The electron density can be approximated to an integration to the peak of the pulse,[14] $\rho(\xi) = [g(\xi)\beta^{(k)}|E|^{2k}]/(K\hbar\omega)$, where $g(\xi) = 0.5(\xi_{min}+\xi)$ and ξ_{min} is a cutoff determined by the initial pulse. The loss was not considered, for simplicity. So the dependence of the spot size of beam a on the distance of propagation, z, can be deduced from Eqs. (1) and (2) by the method introduced in Ref. 11:

$$\frac{k}{2}\left(\frac{da}{dz}\right)^2 + U(a,\tau) = 0, \quad (3)$$

where

$$U(a,\tau) = V(a,\tau) - V(a_0,\tau) - (ka_0{}^2)/(2f^2), \quad (4)$$

$$V(a,\tau) = \frac{2}{ka^2} + \frac{\sigma\omega\tau'\tau_0\beta^{(K)}g(\tau)(2P_{in})^K}{2K\hbar\omega\pi^Ka^{2K}} \times \exp(-2K\tau^2) - \frac{2k_0n_2P_{in}}{\pi a^2}\exp(-2\tau^2),$$

$$V(a_0,\tau) = \frac{2}{ka_0{}^2} + \frac{\sigma\omega\tau'\tau_0\beta^{(K)}g(\tau)(2P_{in})^K}{2K\hbar\omega\pi^Ka_0{}^{2K}} \times \exp(-2K\tau^2) - \frac{2k_0n_2P_{in}}{\pi a_0{}^2}\exp(-2\tau^2),$$

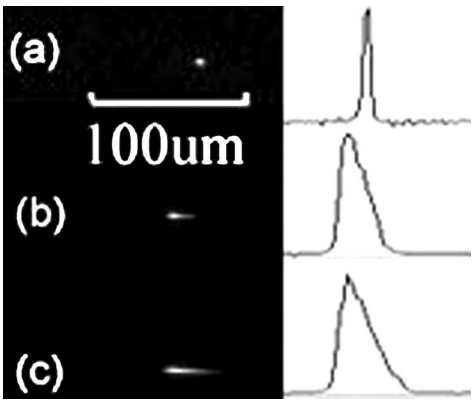

Fig. 4. Photomicrographs and on-axis relative intensities of the plasma luminescence at different pulse energies: (a) 0.24 μJ, (b) 0.64 μJ, (c) 0.92 μJ.

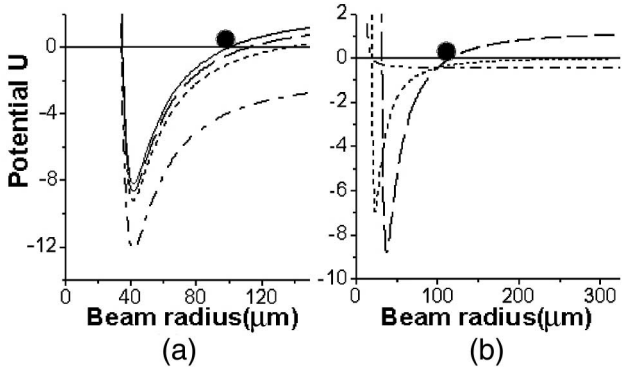

Fig. 5. Profiles of the potential well in Eq. (4) with different focal lengths and single-pulse input energies: (a) $f = \infty$ (solid curve), $f = 3$ cm (dashed curve), $f = 2$ cm (dotted curve), and $f = 1$ cm (dashed–dotted curve). Initial beam radius $a_0 = 0.01$ cm, $P_{in} = 10P_{cr}$. (b) $P_{in} = 8P_{cr}$ (dashed curve), $P_{in} = 3P_{cr}$ (dotted curve), and $P_{in} = P_{cr}$ (dashed–dotted curve). Initial beam radius $a_0 = 0.01$ cm, $f = 3$ cm.

where $\tau = \xi/\tau_0$, P_{in} is the peak input power, and a_0 is the initial beam radius.

Equation (3) shows that the relationship between the spot size of the beam and the distance of propagation is the same as the dependence of the position of a classical particle on the time variable when it is moving in a potential well. The profiles of the potential well with different NAs of the objective are shown in Fig. 5(a).

We can take the beam radius, a, as the position of the particle, in which case $(k/2)(da/dz)^2$ is the kinetic energy of the particle and the initial kinetic energy of the particle is $(ka_0^2)/(2f^2)$. From Eq. (4), it can be deduced that, if $(ka_0^2)/(2f^2) > |V(a_0, \tau)|$, the potential profiles cross at two points in the line with zero potential. That the profiles cross means that the particle will oscillate in the potential well and the position of particle, that is, the beam radius, a, will undergo oscillation, shown as $f = \infty$, $f = 2$ cm, and $f = 3$ cm in Fig. 5(a). Otherwise, $(ka_0^2)/(2f^2) > |V(a_0, \tau)|$, and the particle will reach the minimum position first and then escape to infinity. This means that the beam radius will focus and then diffract, shown as $f = 1$ cm. As we know, the NA of the objective is $a_0/(f^2 + a_0^2)^{1/2}$. Thus we can get a critical NA, N_{cr}, from $(ka_0^2)/(2f^2) = (kN_{cr}^2)/(2 - 2N_{cr}^2) = V(a_0, \tau)$. If the NA of the objective is larger than N_{cr}, no oscillation behavior occurs. As the NA is smaller than N_{cr}, the radius of the beam will oscillate.

Figure 5(b) shows the profile of the potential well with different input energies. For $P_{in} = 8P_{cr}$ and $P_{in} = 3P_{cr}$, the profiles cross at two points on the zero potential line, so the particle will oscillate, and this oscillation shows a refocusing effect of the laser beam. However, for $P_{in} = P_{cr}$, the beam is focused once and is then diffracted. Furthermore, from Fig. 5(b), we find that the higher the input energy of the pulse, the shorter the cycle of beam oscillation, which could explain the unequal space among the peaks in Figs. 3(c) and 3(d). In Fig. 3(c), the distance between the second and the third peaks is larger than that between the first and the second peaks because of energy attenuation resulting from the multiphoton ionization and absorption of the plasma.

In summary, multiple foci have been observed when we focused a single femtosecond laser pulse into fused silica. The dependences of refocusing on the pulse energy and the NA of the microscope objective were studied. When the input-pulse energy was lower, the beam was focused only once during pulse propagation for all the objectives. As the power of the incident pulse was increased, the beam took on multiple foci behavior for objectives with NAs of 0.15 and 0.40. A filament was formed instead of multiple foci for an objective with a NA of 0.85 or larger. A model in which the propagation is analogous to the movement of a classical particle in a potential well represents a qualitative explanation of the experimental results.

This work was supported by National Key Basic Research Special Foundation grant G1999075207 and by the National Natural Science Foundation of China. H. Jiang's e-mail address is hbjiang@mail.phy.pku.edu.cn.

*Corresponding author. Email: hbjiang@mail.phy.pku.edu.cn.

References

1. A. Braun, G. Korn, X. Liu, D. Du, J. Squier, and G. Mourou, Opt. Lett. **20,** 73 (1995).
2. E. T. J. Nibbering, P. F. Curley, G. Grillon, B. S. Prade, M. A. France, F. Salin, and A. Mysyravicz, Opt. Lett. **21,** 62 (1996).
3. A. Brodeur, O. G. Kosareva, C. Y. Chien, F. A. Ilkov, V. P. Kandidov, and S. L. Chin, Opt. Lett. **22,** 304 (1997).
4. A. Brodeur and S. L. Chin, Phys. Rev. Lett. **80,** 4406 (1998).
5. A. A. Zozulya, Phys. Rev. Lett. **82,** 1430 (1999).
6. A. Talebpour, S. Petit, and S. L. Chin, Opt. Commun. **171,** 285 (1999).
7. K. Yamada, W. Watanabe, T. Toma, K. Itoh, and J. Nishii, Opt. Lett. **26,** 19 (2001).
8. E. Miura, J. Qiu, H. Inouge, T. Mitsayu, and K. Hirao, Appl. Phys. Lett. **71,** 3329 (1997).
9. E. N. Glezer, M. Milosavljevic, L. Huang, R. J. Finlay, T.-H. Her, J. P. Callan, and E. Mazur, Opt. Lett. **21,** 2023 (1996).
10. C. B. Schaffer, A. Brodeur, J. F. Garcia, and E. Mazur, Opt. Lett. **26,** 93 (2001).
11. W. G. Wagner, H. A. Haus, and J. H. Marburger, Phys. Rev. **175,** 256 (1968).
12. M. D. Feit and J. A. Fleck, Appl. Phys. Lett. **24,** 169 (1974).
13. M. Mlejnek, E. M. Wright, and J. V. Moloney, Opt. Lett. **23,** 382 (1998).
14. N. Akozbek, C. M. Bowden, A. Talebpour, and S. L. Chin, Phys. Rev. E **61,** 4540 (2000).